Journal of the Electrochemical Society, Vol. 147, No. 1, 2000, pp. 140-148.
ISSN: (Print 0013-4651) (Online 1945-7111)
DOI: 10.1149/1.1393167
http://www.electrochem.org/
http://scitation.aip.org/JES
http://scitation.aip.org/getpdf/servlet/GetPDFServlet?filetype=pdf&id=JESOAN000147000001000140000001&idtype=cvips&prog=normal

Pit Growth Study in Al Alloys by the Foil Penetration Technique

A. Sehgal,[a] G. S. Frankel,[a,] B. Zoofan,[b] and S. Rokhlin[b]
[a]The Fontana Corrosion Center, Department of Materials Science and Engineering, and
[b]Department of Industrial, Welding and Systems Engineering, The Ohio State University

The foil penetration technique was used to study pit growth in AA1100-O and AA2024-T3. Preliminary work on AA1100-O foils of different thicknesses indicated that the pit growth rate increased with increasing applied potential, suggesting that pit growth was not under transport control. Foil penetration experiments were also carried out on AA2024-T3 foils of a given thickness, at open circuit as well as anodic potentials. Dichromate ions and other oxidizing agents were added to some test solutions. Dichromate ions were shown to have little influence on the pit growth rate at controlled anodic potentials, even when added in large concentrations. However, dichromate ions effectively inhibited pitting at open circuit when present in very small amounts. Polarization curves of AA2024-T3 in 1 M NaCl with various additives show a large effect of dichromate ions in the cathodic region and no effect in the anodic region. These observations suggest that chromate (or its reduction product) acts as a cathodic inhibitor. Examination of penetrated samples was performed by optical and scanning electron microscopies, as well as by microradiography.

The foil penetration technique is a simple and direct method of measuring pit growth rate in materials.[1] One can vary the sample thickness, sample orientation, test environment, and applied potential, and determine the kinetics of the fastest growing pit regardless of the pit growth path. In the original experiment by Hunkeler and Böhni,[1] pit penetration times were determined for Al foils of different thicknesses (0.05-0.20 mm) that were potentiostatically held at anodic potentials. Their Al foil working electrode was mounted onto the cell wall, and was backed by a Cu foil maintained at +12 V relative to the working electrode (WE), with a piece of paper separating the two metal foils. The instant of pit penetration, through the Al foil, was detected as the pit electrolyte wetted the paper, thus reducing the resistance between the Al and Cu foils and triggering a timer.

Hunkeler and Böhni found the pit growth rate (the inverse slope of the penetration time/foil thickness relation) increased linearly with increasing potential, suggesting ohmic or mixed ohmic/charge-transfer control of pitting.[1] These experiments were repeated by Cheung *et al.*[2] with some minor variations (Table I). Cheung *et al.* found the pit growth rate to be independent of the applied potential, indicating that the pit was under diffusion control.[2] Cheung *et al.* indicated that Hunkeler and Böhni's results were tainted by crevice corrosion. They suggested that crevice corrosion of the sample increased the dissolution rate of the Al foils and led to quicker pit penetration.[2]

Table I. Foil penetration conditions for Al 1100-O experiments by various research groups.

Conditions	Hunkeler and Böhni[1]	Cheung *et al.*[2]	This work
Specimen			
Purity	>99.2%	99%	99.24%
Thickness	0.05, 0.100, and 0.200 mm	0.050, 0.075, 0.100, 0.125, 0.150, and 0.450 mm	0.050, 0.076, 0.102, and 0.127 mm
Polishing	??	As received; reflective finish	As received; reflective finish
Cleaning	Ultrasonic with water, acetone and benzene	??	Methanol and dried in argon
Orientation	Vertical	Vertical	Horizontal
Deaeration			
Electrolyte	✓	×	✓
Cell	✓	×	✓
Electrolyte	1, 0.1, 0.01, and 0.001 M NaCl + NaOH to make a pH 11 solution	0.10 and 0.01 M NaCl	0.10 M NaCl
Avesta modification	×	✓ Distilled water at 1 mL/h	×
Surface activation	??	??	1 N NaOH for 20 s; 300 mV above E_{pit} for 1 s to initiate pit(s).
Applied potential	Cl^-:1 M (−750, −720, −650) 10^{-1} (−640) 10^{-2} (−565, −480, and −430) 10^{-3} (−470)	Cl^-: 10^{-1} M (−565) 10^{-2} (−565, −545, and −500)	Cl^-: 10^{-1} M (−500, −565, and −640)

In this paper the issue of the rate-controlling step for pit growth in Al foils is reexamined. Also, pit growth in AA2024-T3 foils is studied at anodic potentials and open circuit in 1 M NaCl solutions containing different amounts of inhibitors ion (dichromate) and oxidizers (hydrogen peroxide and sodium persulfate). The foil penetration method is a powerful tool for measuring pit growth rates, which are important for design considerations, and for determining the mechanism of pitting inhibition.

Experimental

Foil penetration experiments were performed using an approach similar to that developed by Hunkeler and Böhni.[1] The test foil/WE was pressed against an O-ring at the bottom of a Plexiglas cell. A piece of filter paper and a Cu foil were positioned between the sample and a Plexiglas backing plate. The penetration detection circuit used in this work, shown schematically in Fig. 1, is similar to that described by Hunkeler and Böhni.[1] A voltage comparator was used to detect pit penetration. The Cu foil was held at +12 V relative to the foil at ground with the paper as isolation. When a pit penetrated through the foil WE, the paper was wetted by the pit electrolyte and its resistance decreased. The dry resistance of the filter paper was greater than 200 MΩ, the limit of our multimeter. The voltage comparator was set at 6.2 V; when the paper resistance fell below the calculated critical resistance of M10.7 Ω, the comparator switched the relay, shut off a timer, and turned on a red LED (light-emitting diode) and a 98 dB alarm (not shown in Fig. 1). In addition, triggering of the detection system disconnected the cell counter electrode, which minimized corrosion of the WE prior to disassembly of the cell for tests performed at an applied anodic potential. Furthermore, a 10 Mil resistor between the Cu and Al foils limited the current flow between them to 1.2 μA after penetration. A discussion of the influence of the set point voltage on the measured detection time is given in the results section.

AA2024-T3 sheet (Cu 3.8-4.9%, Mg 1.2-1.8%, Mn 0.30-0.90%, Si 0.50 Max %, Fe 0.50

Max %, Zn 0.25 Max %, Ti 0.15 Max %, Cr 0.10 Max %, and other elements total 0.15 Max %) of thickness 0.216 mm was purchased from Heinzen Metals, Inc., Palatine, IL. AA1100-O samples (Al 99.24%, Cu 0.15%, Fe 0.50%, Si 0.11%, Mn 0.004%, Mg < 0.001%, Zn < 0.006) of various thicknesses (0.051, 0.076, 0.102 and 0.127 mm) were bought from Midwest Metals, Westlake, OH. The AA1100-O samples were degreased in methanol and argon dried. To ensure similar surface conditions for all the AA1100-O specimens, they were immersed in 1 M NaOH for 20 s and subsequently cleaned with water and argon dried. The AA2024-T3 samples were polished in methanol to 800 grit prior to use. Water-polished samples were severely pitted after polishing, whereas samples polished in methanol were less attacked. The change in thickness as a result of polishing was found to be less than 10 μm.

Owing to the stochastic nature of pitting corrosion, replication of the foil penetration experiments is required. In order to facilitate replication, an experimental apparatus allowing eight simultaneous experiments on different samples in different cells was constructed. A Gamry, Instruments (Warminster, PA) PC-3 potentiostat and multiplexer, along with CMS 208 and custom-made software packages purchased from Gamry were used to control the potential (except in open-circuit experiments) and acquire data from all cells simultaneously.

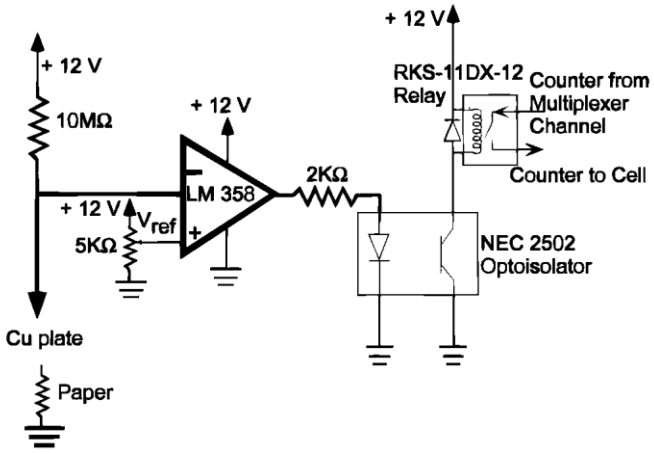

Figure 1. A schematic of the detection circuit.

High-purity reagents and Millipore water were used to make up solutions. All experiments were conducted at room temperature. Argon and oxygen gases were used in the AA1100-O experiments and the AA2024-T3 experiments, respectively, to aid convection in the cell and, in the case of oxygen, to maintain a constant supply of cathodic reactant.

Some experiments were performed at open circuit so that the cathodic reactions would occur on the sample surface instead of at the counter electrode, as in the case of potentiostatic control. To accelerate the rate of pitting at open circuit, hydrogen peroxide or sodium persulfate was added to the solution in some experiments. In order to replenish the oxidizing agent and minimize a decrease in its activity, an eight-channel Ismatec (Zürich, Switzerland) peristaltic metering pump was used to pump stock solution into each cell from an ice-chilled reservoir. The reservoir was kept cold in an attempt to slow the decomposition of the oxidizers. The tubing length (from the reservoir to each cell) was over 2.4 m (8 feet) and the pumping speed was slow (about 3.75 mL/h) so the solution is believed to have been at room temperature when it entered the cell. Solution was removed from the cells every 12 h to prevent electrolyte overflow.

Crevice corrosion was minimized by using either a knife-edge Teflon O-ring (EG&G Princeton Applied Research, Princeton, NJ) or Apiezon-W black wax to define the exposed specimen area. A schematic of the lower part of the cell is shown in Fig. 2.

For anodic potentiostatic pitting experiments, a Pt counter electrode and SCE reference electrode were used in each cell. For open-circuit pitting experiments, the Pt counter electrode was removed from the electrolyte to prevent it from catalyzing the oxidizer breakdown. In addition, the cell body, cell cover, and the reservoir were covered to decrease light-assisted decomposition of the oxidizer.

In the foil penetration experiments, the intent was to study pit growth, not pit initiation. Therefore, all samples were anodically polarized to 300 mV above the pitting potential (in the given electrolyte) for 1 s to initiate pits, followed by an immediate change to the applied potential or to open circuit. Longer initiation times were not used because they resulted in decreased pit penetration times. The minimum time allowed by the software package for simultaneous polarization of all cells was 1 s, so that was the value used in all experiments. The cells were assembled, gas flow started in each cell, solution added to the cells, and the timer started followed by potentiostatic polarization for 1 s to initiate pits. The time elapsed between adding solution to the first cell to the application of the pit initiation potential was about 2.5 min.

Microradiographic analysis was performed on some penetrated AA2024-T3 foils. This technique provides a description of the corrosion attack morphology through the thickness of the sample in a nondestructive manner. It combines the sensitivity of X-rays to discontinuities and/or thickness change with a microfocal X-ray source to increase resolution. With this technique, very small (<10 μm) pits have been detected[3] A Feinfocus 225 kV X-ray unit (Garbßsen-Berenbostel, Germany) with a 5 μm focal size was used as the X-ray source. A precise positioning system with three linear (2 μm resolution) and one rotating (0.01° resolution) computer-controlled axes was used to control sample positioning. Eastman Kodak AA film was placed in front of the image intensifier. A Data Translation frame grabber (DT3155) was used to digitize the X-ray films. More details about microradiography, the setup, and procedure are reported in Ref. 3.

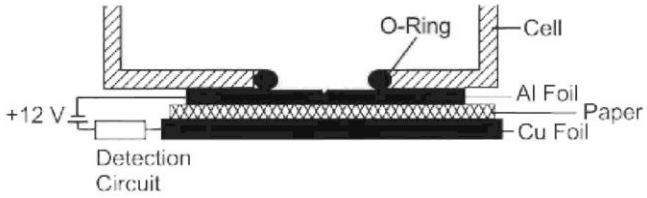

Figure 2. Schematic of the lower part of cell used for foil penetration experiments.

For pitting potential and polarization curve determination, each specimen was held at open circuit for 1 h to allow stabilization. Pitting potential was determined by applying 10 mV potentiostatic steps and holding for 5 min. The potential at which the current increased (at the end of the hold time) was considered to be the pitting potential. Anodic and cathodic polarization curves were measured on separate samples by scanning the potential at 0.5 mV/s from the open-circuit potential, and the average of three curves is reported.

Results and Discussion

Accuracy of penetration time measurement.—In the experimental section, it was stated that the set point of our detection circuit was 6.2 V. Based on tests on samples with intentional pinholes, this set point allowed detection of penetrated pits less than 15 μm in size. A higher set point voltage would cause the circuit to be tripped at a higher paper resistance, *i.e.*, with a smaller amount of electrolyte. It could be argued that smaller pits (and shorter measured penetration times) would be detected if our detection set point was set at a higher voltage. To address this concern, eight detection circuits with different set points were connected to one cell. The sample was a 0.216 mm thick AA2024-T3 sample exposed to an oxygen-bubbled 1 M NaCl + 5.0 vol % H_2O_2 electrolyte and pitted at open circuit after a 1 s activation to initiate pits. The results are shown in Table II. The penetration time is nearly the same as the mean of 35 other experiments (performed with a 6.2 V set point). The variation in detection time for all the circuits was less than 10 s. To rule out any interference of the detection circuits with each other, they were sequentially turned off starting with the highest set point first until only circuit 7 was left on. Circuit 7 could detect the penetration event unambiguously as all attempts to reset circuit 7 failed (the cell was still assembled with the penetrated sample in place); it tripped repeatedly, regardless of any, some, or all of the other detection circuits being on. This experiment proves that the paper resistance decreases very quickly after sample penetration as it is wetted with pit solution and that the chosen set point voltage can detect the penetration quickly and give a very accurate penetration time. Neither of the previous research groups that used the foil penetration technique reported the smallest pit size detectable with their detection circuits.[1,2] However, based on these results, variations in the detection circuit design or set point probably had little influence and cannot explain the differences in their results.

Pit growth in AA1100-O.—Preliminary penetration experiments were performed on AA1100-O foils of different thicknesses (0.05 — 0.127 mm) at different potentials (−500 to −640 mV SCE) in a deaerated 0.10 M NaCl solution. The experimental conditions are summarized in Table I, and the results are shown in Fig. 3. The pit growth rate at −500 mV SCE is somewhat higher than that at −565 mV SCE, and much higher than that at −640 mV SCE. Since the pit growth rates increased with applied potential in the range studied, pit growth rate was apparently not under transport control but was limited by a combination of ohmic and charge-transfer effects. This finding supports the results of Hunkeler and Böhni[1] and is contrary to those of Cheung *et al.*[2] for very similar experimental conditions (but not identical, see Table I).

Table II. Details of the detection circuit accuracy measurements. All eight circuits were connected to the same cell in which a 0.216 mm thick AA2024-T3 was open-circuit pitted in oxygen-bubbled 1 M NaCl + 5.0 vol % H_2O_2.

Circuit No	Set point voltage[a]	Paper resistance just before circuit detects penetration	Detection time
1	10.500	70.00 MΩ	1.8 h
2	10.000	50.00 MΩ	5 s after circuit 1
3	9.500	38.00 MΩ	8 s after circuit 1
4	8.500	24.29 MΩ	8 s after circuit 1
5	8.000	20.00 MΩ	8 s after circuit 1
6	7.500	16.67 MΩ	8 s after circuit 1
7	6.200	10.69 MΩ	8 s after circuit 1
8	7.000	14.00 MΩ	8 s after circuit 1

[a] Maintained at ±0.002 V of set point voltage.

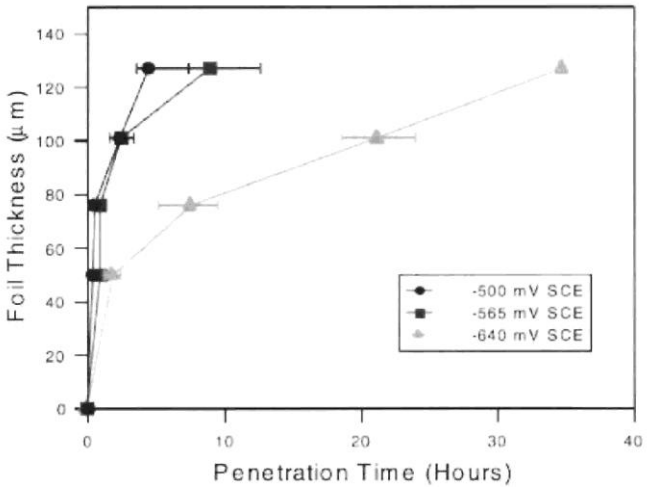

Figure 3. Influence of applied potential on pit growth in AA1100-O foils.

Pit Growth in AA2024-T3.—Further work focused on the influence of inhibitor ions on localized corrosion of AA2024-T3. The experiments were performed on 0.216 mm thick AA2024-T3 in 1 M NaCl base solutions with or without dichromate ions. This sheet was the thinnest 2024-T3 that was commercially available. Thin, as-received sheet was used instead of reducing the cross section of thicker material in order to avoid artifacts that may be generated by the various thinning processes. The penetration time for samples of only one thickness does not provide the full time-dependent pit growth rate but does allow comparison of the effect of different environments.

Polarization curves were measured on the AA2024-T3 samples in 1 M NaCl base solution containing a range of dichromate concentration (Fig. 4a). In agitated, oxygen-saturated 1 M chloride solution, the corrosion potential of this alloy was essentially pinned at the pitting potential as a result of the nonpolarizability of the pitting reaction. The nominal current density increased sharply at potentials above the open-circuit potential owing to pit growth. The cathodic region of the polarization curve shows a limiting current density of about 5×10^{-5} A/cm^2 that is

probably associated with oxygen reduction. Since the electrode was stationary and agitation provided only by gas bubbling, the hydrodynamics were not well controlled. As a result, there is no direct proof that the current was limited by diffusion of oxygen.

Figure 4a shows that the addition of dichromate ions had little influence on the corrosion potential and current densities in the anodic region. The addition of relatively small concentrations of dichromate (10^{-5}-10^{-3} M), however, resulted in a significant decrease in the current in the cathodic region. This is interesting since the Cr^{6+}/Cr^{3+} reversible potential, is quite high relative to the open-circuit potential, and chromate is generally considered to be an oxidizing agent. Changes in solution pH or in oxygen solubility with dichromate addition cannot explain the large decrease in cathodic current.

To further investigate the apparent lack of influence of dichromate ions on the anodic part of the AA2024-T3 polarization curves, potentiostatic anodic foil penetration experiments were carried out at −550 mV SCE in 1 M NaCl base solutions with and without dichromate ions. This potential is only about 50 mV more noble than the open-circuit/pitting potentials. The results are shown in Fig. 5. The foil penetration time was about 2 h at open-circuit in 1 M chloride solutions containing up to 0.1 M dichromate. The error bars show the scatter in the measurements and reflect the stochastic nature of pit growth. In 1 M NaCl + 1 M $Na_2Cr_2O_7$, the time for penetration of the 0.216 mm thick foil increased to a value approximately twice that of the other solutions. Relative to the effectiveness of dichromate under other conditions, this decrease in the average pit growth rate by a factor of two is a very small effect. These findings are in accordance with the anodic portions of the polarization curves, which were essentially identical for solutions containing dichromate concentrations from 0 to 1 mM dichromate. These results are also in accordance with reported literature showing that in potentiostatically controlled experiments, relatively large amounts of chromate are needed to influence pit growth and pitting potential of Al in chloride solutions.[1,4,5] The large dichromate:chloride ratios needed to effect small changes in pit growth rates at a small applied anodic potential suggests that anodic inhibition is not the mechanism by which dichromate reduces the localized corrosion of Al and Al alloys.

The major effect of dichromate in the polarization curves shown in Fig. 4 is in reducing the rate of the cathodic reaction. More correctly, it is likely that the reduction product of dichromate, perhaps Cr_2O_3, is the cathodic inhibitor. A cathodic inhibitor reduces corrosion by limiting the available cathodic current and thereby slowing the anodic dissolution reaction. Given the relative nonpolarizability of the pitting reaction, it may be considered that pitting at open circuit is under cathodic control; pits grow as fast as cathodic current is supplied to them and will cease growing if the available current is insufficient for them to grow at a minimum rate for pit stability. Therefore, it is not surprising that a cathodic inhibitor would be particularly effective at reducing open circuit pitting. Furthermore, studying the effects of cathodic inhibitors by potentiostatically controlled experiments at anodic potentials is not useful as the potentiostat provides whatever current is needed for the reaction to proceed, and the balance between the anodic and cathodic reactions is not maintained. It is critical to investigate pitting under open-circuit conditions in order to observe and study the influence of cathodic inhibitors.

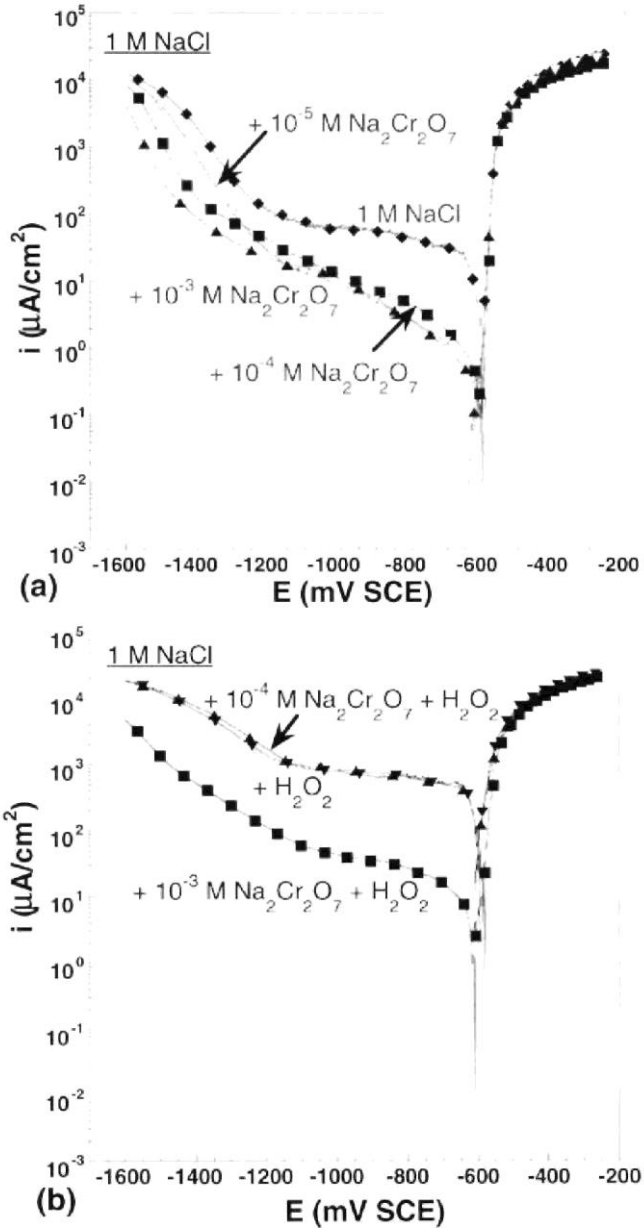

Figure 4. Polarization curves of AA2024-T3 in an aerated, oxygen-stirred 1 M NaCl base solution with (a) dichromate and (b) 0.3 vol % peroxide and dichromate added to the solution.

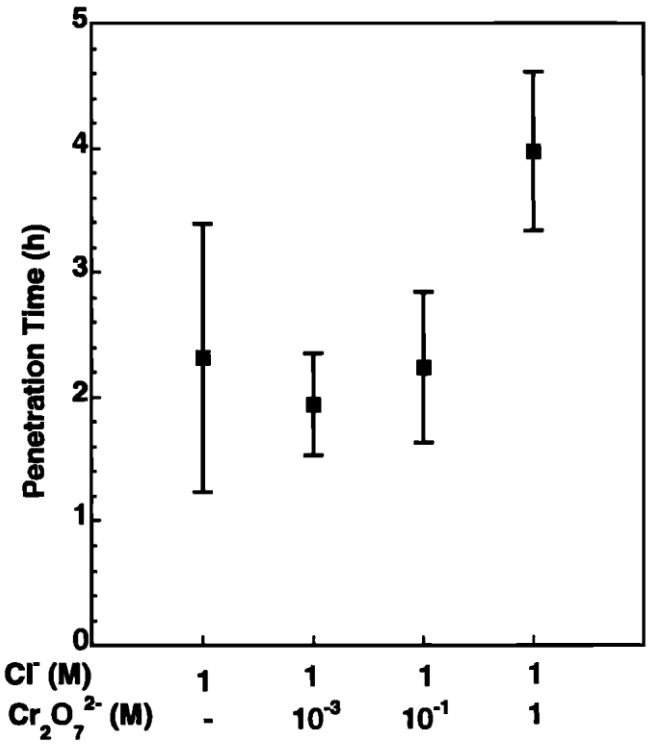

Figure 5. Average foil penetration time for 0.216 mm thick AA2024-T3 foils potentiostatically controlled at —550 mV SCE in oxygen-bubbled 1 M NaCl base solutions containing different amounts of dichromate ions, as shown on the *x* axis. Bars indicate standard deviation of results.

Subsequent experiments were performed at open circuit. The average penetration time through 0.216 mm thick AA2024-T3 foils at open circuit in oxygen-bubbled 1 M NaCl was 50.6 ± 23.4 h (Table III). The average potential at the moment of penetration was —614.5 ± 4.9 mV SCE. It should be noted that the penetration time of 50.6 h represents the average of the samples that were penetrated after 168 h of exposure. Five of the ten tested samples did not penetrate in this time. Considering the influence of the unpenetrated samples, the real average penetration time is much larger than 50.6 h. However, as shown later, the 50.6 h value is almost an order of magnitude larger than the results reported for the oxidizer-containing solutions. The scatter in the data is a result of the fact that AA2024-T3 is a wrought alloy. Pits that grow intergranularly in a wrought structure may be deflected from penetrating the foil in the short transverse direction. This point is discussed further.

Pit penetration through thin AA22024-T3 foils took over 2 days on average in a pure chloride solution, and it was expected that penetration times would increase with inhibitor addition to the base solution. In order to make open-circuit measurements on samples in inhibited solutions in a reasonable amount of time, oxidizing agents were added to the solution.

Table III. Open-circuit foil penetration results of activated 0.216 mm thick AA2024-T3.

Identifier	Solution			Solution circulation	O_2 bubbling	Results	
	Cl^-	$Cr_2O_7^{2-}$	Oxidizer			T_p (h)	E_p (mV SCE)
a	1 M	—	—	✗	✓	50.64 ± 23.42[a]	−614.50 ± 4.95
	1 M	—	5.0 % H_2O_2	✗	✓	2.69 ± 0.07	−471.29 ± 8.69
	1 M	10^{-4} M	5.0 % H_2O_2	✗	✓	2.20 ± 0.29	−463.00 ± 14.06
b	1 M	—	0.3 % H_2O_2	✗	✓	7.00 ± 6.69	−604.43 ± 14.67
c	1 M	10^{-4} M	0.3 % H_2O_2	✓	✓	6.60 ± 3.51	−610.00 ± 17.93
d	1 M	10^{-3} M	0.3 % H_2O_2	✓	✓	All 7 cells unpenetrated after 137 h	All 7 cells unpenetrated after 137 h
e	1 M	10^{-3} M	—	✓	✓	All 7 cells unpenetrated after 205 h	All 7 cells unpenetrated after 205 h
f	1 M	—	5×10^{-2} M $Na_2S_2O_8$	✓	✓	4.70 ± 1.26	−606.67 ± 6.25
g	1 M	10^{-4} M	5×10^{-2} M $Na_2S_2O_8$	✓	✓	All 7 cells unpenetrated after 142 h	All 7 cells unpenetrated after 142 h
h	1 M	10^{-6} M	5×10^{-2} M $Na_2S_2O_8$	✓	✓	5.01 ± 1.03	−608.86 ± 3.39

[a] Only five of the ten tested samples penetrated after 168 h. Data reported are the average of the five penetrated samples; in all other solutions, all the other tested samples either penetrated or did not penetrate.

Hydrogen peroxide was the first oxidizing agent investigated. A peroxide concentration of 0.3 vol % is used in ASTM standards for testing Al alloys,[6] and has been used in experiments on AA2024 and other Al alloys.[7] The effect of 0.3 vol % H_2O_2 on the AA2024-T3 polarization curves in 1 M NaCl is shown in Fig. 4b. Like dichromate, the addition of 0.3% peroxide had little effect on the corrosion potential, which was still effectively pinned at the pitting potential, or on the anodic region of the polarization curves. However, the addition of peroxide greatly increased the cathodic reaction compared to oxygenated chloride solutions. This is the expected influence of an oxidizing agent and is in contrast to the effect of addition of small amounts of dichromate ions.

In the presence of 0.3% H_2O_2, the addition of 10^{-4} M dichromate had no effect on the cathodic part of the polarization curve, which is different than the behavior in the absence of peroxide. However, the addition of 10^{-3} M dichromate to the peroxide + chloride solution reduced the cathodic current by over an order of magnitude. In other words, at these concentrations, dichromate acted as a cathodic inhibitor, even in the presence of peroxide. However, more dichromate was required to have an effect relative to the peroxide-free case. As in the peroxide-free solutions, dichromate had no influence on the corrosion potential or the anodic branch of the curves.

The effect of peroxide on open-circuit foil penetration rate is shown in Fig. 6 and Table III. The addition of 0.3 vol % H_2O_2 to an oxygenated 1 M NaCl solution reduced the average penetration time from greater than 50 h to 7.0 ± 6.7 h. The addition of peroxide to the test solution therefore allowed for open-circuit penetration experiments to be accomplished in a reasonable amount of time. Figure 6 also indicates the average corrosion potential at the start of the experiment and at the point of penetration. In cases where the samples did not penetrate, open-circuit values 72 h into the experiment are reported. The potentials in 0.3 vol % H_2O_2 + 1 M NaCl were only slightly higher than those measured in the pure chloride solution.

The addition of 10^{-4} M dichromate to the peroxide-containing solution had an insignificant influence on the penetration time and the potentials. This may be predicted from the

polarization curves, where 10^{-4} M dichromate also had an insignificant effect (Fig. 4b). However, addition of 10^{-3} M dichromate to the 0.3 vol % H_2O_2 + 1 M NaCl solution effectively eliminated pitting, as no cells penetrated after prolonged exposure (137 h or more), and no signs of attack were seen on the samples after disassembling the cells. This response might also be predicted based on the polarization curves. The addition of 10^{-3} M dichromate to 1 M NaCl also eliminated pitting at open circuit. As described previously, pit growth at open circuit is cathodically limited; pits will grow as fast as the current can be consumed by a cathodic reaction and will not grow if the extent of cathodic reaction is insufficient.

This inhibition of pitting at open circuit provided by small amounts of dichromate is in stark contrast to the behavior under potentiostatic conditions at slightly elevated potentials described previously, where large concentrations of dichromate were needed to have a small effect. The influence of chromate on pitting of Al and Al alloys has been studied by others and the amount of chromate ions needed to influence pitting depends upon the amount of chloride present and the stages of pitting corrosion under study. The growth rates of large pits in 0.2 mm thick foils, under potentiostatic control, in 10^{-2} M NaCl was not changed unless 0.1 M $NaCrO_4$ was added, a 10:1 chromate:chloride ratio.[1] The pitting potential of Al was found to increase only if the chromate:chloride ratio was about 1:4 in a 10^{-2} M NaCl solution.[4] Metastable pitting of Al was strongly reduced when the chromate:chloride ratio was only 1:40 in a 10^{-3} M NaCl solution.[8] Extended exposure of AA2024-T3 to small amounts of chromate ($<10^{-4}$ M) in 0.1 M chloride at open circuit has been shown to have a large beneficial effect on pitting resistance.[9] So the amount of chromate ions needed to affect pitting seems to increase as the stage of pits increases from metastable to critically stable to deep pits.

It is interesting to note that the cathodic polarization curve for the 1.0 M NaCl + 0.3% H_2O_2 + 10^{-3} M $Na_2Cr_2O_7$ is only slightly below that for 1.0 M NaCl alone. However, severe pitting occurred in the pure chloride solution, with a 51 h mean penetration time, whereas pitting was effectively inhibited in the solution with peroxide and dichromate. It is clear that the polarization curves alone cannot fully predict the open-circuit pitting behavior. This point is discussed more near the end of this section.

Experiments were also performed with additions of persulfate instead of peroxide as the oxidizing agent. Peroxide is quite unstable and readily decomposes. Persulfate is much more stable, having a half-life in water of about 1 year.[10] Even in water containing salts, persulfate decomposition should result in gaseous products (oxygen, sulfur (di/tri)oxide).[10-12] No gas bubbles resulting from persulfate decomposition were observed either in the reservoir or the cell. Furthermore, peroxide reduction can result in significant pH increases at the sample surface, creating an artifact, while persulfate simply reduces to sulfate with no change in pH. Sulfate has been reported to inhibit pitting of Al,[4,13] but experiments with intentional additions of sulfate to the chloride + persulfate solution had no effect on the foil penetration time.

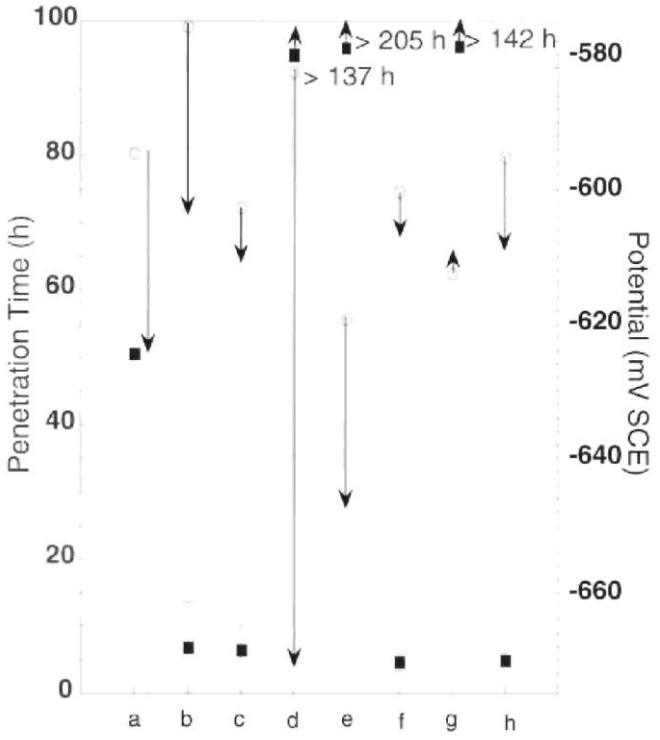

Figure 6. Average foil penetration time and potential for 0.216 mm thick AA2024-T3 foils pitted at open circuit in different oxygen-bubbled solutions. The solution compositions for a-h are identified in Table III. The squares represent the mean penetration time, and the bars indicate the standard deviation. For the 1 M NaCl solution (solution a), the data reported are for five of the ten samples that penetrated in 168 h; all the other tested samples either penetrated or did not penetrate. Circles represent average potential at the start of the test, end of arrows from circles represent average potential at penetration (or after 72 h for unpenetrated samples).

Polarization curves for AA2024-T3 in 1 M NaCl solutions containing sodium persulfate are shown in Fig. 7. Like peroxide, persulfate additions to chloride resulted in an increase in the cathodic currents with little influence on the corrosion potential or anodic currents. In the presence of 0.05 M $Na_2S_2O_8$, dichromate additions resulted in large decreases in the cathodic currents. The foil penetration results displayed the same trend as shown by peroxide additions. Addition of oxidizer (0.05 M $Na_2S_2O_8$) only to the base 1 M NaCl solution decreased the penetration time to 4.70 ± 1.26 h (from >51 h) and very small additions of dichromate ions (10^{-4} M $Na_2Cr_2O_7$ to 1 M NaCl + 0.05 M $Na_2S_2O_8$) effectively killed pitting. Figure 7 shows that the cathodic current density in dichromate-containing solution was similar to that in 1 M NaCl + 0.05 M $Na_2S_2O_8$ only when the dichromate concentration was as low as 1×10^{-6} M. Open-circuit pitting in an oxygen-stirred 1 M NaCl + 0.05 M $Na_2S_2O_8$ + 10^{-6} M $Na_2Cr_2O_7$ solution gave penetration times of 5.01 ± 1.03 h, which are identical to penetration rates reported in the 1 M NaCl + 0.05 M $Na_2S_2O_8$ solution, 4.70 ± 1.26 h. The polarization curves are successful at qualitative prediction of the foil penetration time, with the exception of the 1.0 M NaCl + 0.3% H_2O_2 + 10^{-3} M $Na_2Cr_2O_7$ solution in which no pitting occurred even though its cathodic polarization curve was only slightly below that for the base 1.0 M NaCl solution. Careful examination of the polarization curves reveals that, for foil penetration to occur after exposure to a particular solution, the nominal corrosion current density in that solution, which is determined by the limiting cathodic current, needs to be higher than 20-30 μA/cm^2. Solutions in which the

corrosion rate was below 20 μA/cm^2 could not sustain stable pit growth at open circuit. This observation of a critical nominal current density needs to be verified by using other solutions and forming a larger database to support or reject or refine the critical corrosion rate value.

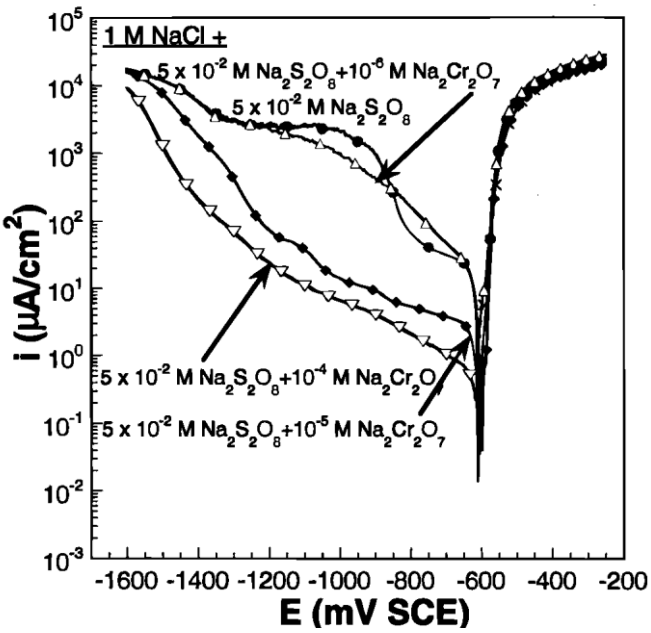

Figure 7. Polarization curves of AA2024-T3 in an aerated, oxygen-stirred 1 M NaCl base solution containing different amounts of persulfate and dichromate ions.

Pit characterization.—The pits that formed in these wrought AA2024-T3 foil samples were extremely convoluted in shape. For instance, no light is transmitted through penetrated samples that contain through-pits. As a result, characterization of pit morphology by optical or scanning electron microscopy (SEM) is extremely difficult. Clearly, any pit depth measurement made from the top of a pit would be erroneous given the convoluted nature of the pits. Careful sectioning of pits might reveal a portion of the convoluted shape, but such an approach is extremely tedious and time consuming. The foil penetration technique has distinct advantages since it senses the penetration time in the direction of the foil thickness regardless of the pit growth path.

An interesting method for quantitative determination of damage to the material is microradiography. Microfocal radiography, a nondestructive inspection technique that has recently been applied to the determination of pit size and depth,[3] was used to characterize the penetrated foil samples. Different projection magnifications were used during microradiography. A small projection magnification (8 times) was used to evaluate the entire area of the corroded surface, and higher projection magnifications in the range of 40-80 times were used to study the penetrated points in some detail. A microradiograph of a penetrated sample is shown in Fig. 8. This sample was exposed at open circuit to 1 M NaCl + 0.3 vol % H_2O_2 + 10^{-4} M $Na_2Cr_2O_7$. It penetrated in 5.1 h and was removed from solution a few hours later. The sharp images can be further magnified optically to improve resolution, providing considerable detail. The low-magnification image in Fig. 8 shows many pits that appear dark. The darkness of the radiograph scales with material loss so that the darkest spots indicate the deepest pits. The exposed area was attacked at many points but observation of the surface by the naked eye and SEM confirmed that

only 1 pit penetrated to the unexposed side. The convoluted nature of that pit is clearly seen by the evidence of lateral spreading and branching. This pit morphology might be expected for a wrought alloy having a directional microstructure with grains elongated in the rolling direction if the attack is intergranular in nature. Pit growth in this study was measured in the short transverse direction, which is perpendicular to the orientation of the elongated grains. The rate of attack in longitudinal directions may be very different.

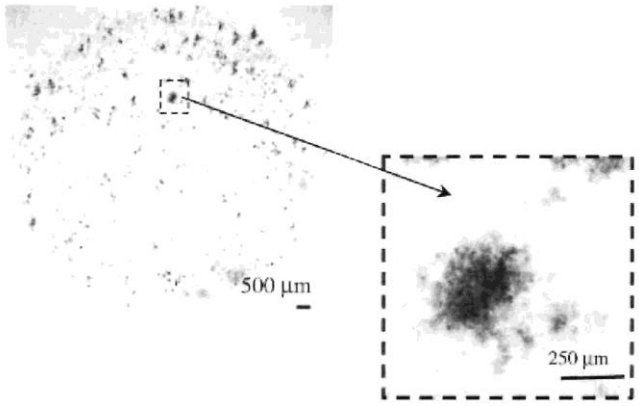

Figure 8. Microradiograph of 0.216 mm thick AA2024-T3 open-circuit pitted in an oxygen-stirred 1 M NaCl + 0.3 vol % H_2O_2 + 10^{-4} M $Na2Cr_2O_7$ solution.

SEM images of the exposed and unexposed sides of the same sample studied by radiography are shown in Fig. 9. The surface exposed to the electrolyte was covered by corrosion products that obscure many of the pits, except at the perimeter. The only pit to penetrate the foil is shown in Fig 9b. Corrosion products filled the pit. Clearly, the microradiographs in Fig. 8 provide a better description of the corrosion attack by detailing the location and spatial distribution of all the pits.

SEM images of a sample that was removed immediately after penetration are given in Fig. 10. This particular sample was pitted at open circuit by exposure to a 1 M NaCl + 5.0×10^{-2} M $Na_2S_2O_8$ solution and penetrated in 3.4 h. The region of attack is much smaller than for the sample in Fig. 9, which sat in the solution for some time after penetration. The penetrating pit in Fig. 10 is seen to be actually three pits that reached the unexposed surface at about the same time, surrounded by corrosion products that charged under the electron-beam. This figure is representative in the fact that all samples removed immediately after penetration have a large penetrating pit with a number of smaller pits close to it. Samples allowed to remain in solution at open circuit after penetration exhibited continued attack. The boundary wall between the individual pits was corroded, resulting in a large pit that is not representative of the multiple pits that initially reached the unexposed surface.

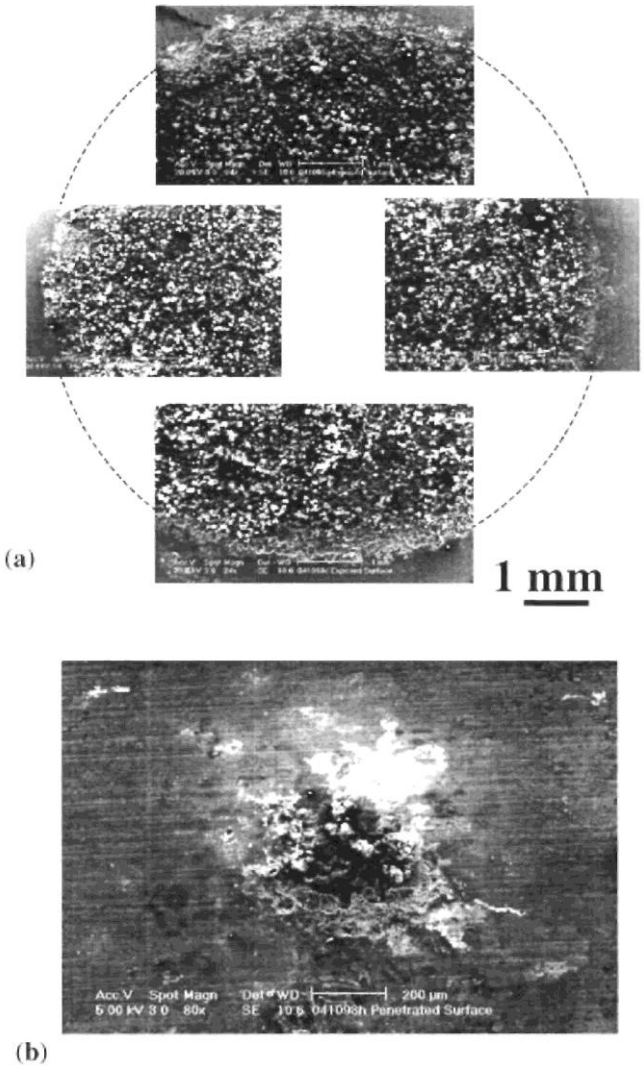

Figure 9. SEM pictures of 0.216 mm thick AA2024-T3 foil open-circuit pitted in an oxygen-bubbled 1 M NaCl + 0.3 vol % H_2O_2 + 10^{-4} M $Na2Cr_2O_7$ solution showing the surface (a) exposed to solution and (b) unexposed surface.

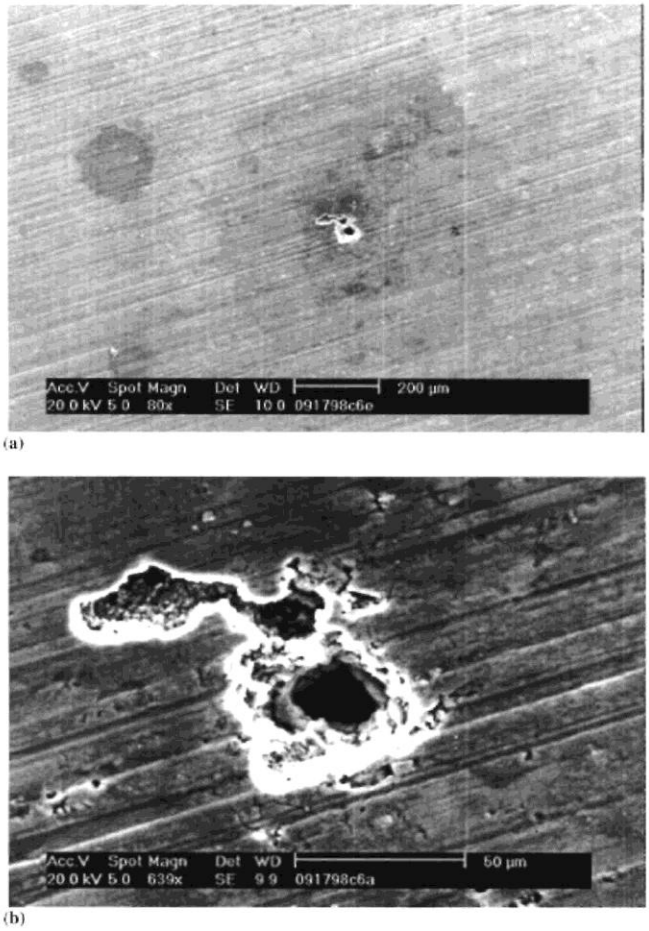

Figure 10. Penetrated pit at the unexposed side of a 0.216 mm thick AA2024-T3 sample, the other side of which was exposed at open circuit to an oxygen-stirred 1 M NaCl + 5×10^{-2} M $Na2S_2O_8$ solution. Note that the features in the lower magnification image are surface stains and do not appear in the microradiograph of Fig. 11.

The microradiograph of this sample is shown in Fig. 11. The penetrating pit is marked by using a thin lead wire. Comparison to Fig. 8 shows that in persulfate solutions the pitting is extremely localized with almost all of the surface unattacked. The tortuous path branching and lateral spreading of the pit is clearly visible in the microradiograph.

Another noteworthy metallographic detail is the morphology of pits generated in the potentiostatically controlled experiments described previously (data of Fig. 5). Figure 12 is an optical photograph of samples pitted at an anodic potential of —550 mV SCE in solutions containing different amounts of dichromate ions. The samples were removed from solution shortly after penetration. The pits are small and uniformly distributed in the sample tested in the 1 M NaCl solution. The pits formed in solutions with increasing concentration of dichromate ion became increasingly distinct. There was less general attack of the region between the pits as a result of protection provided by the dichromate.

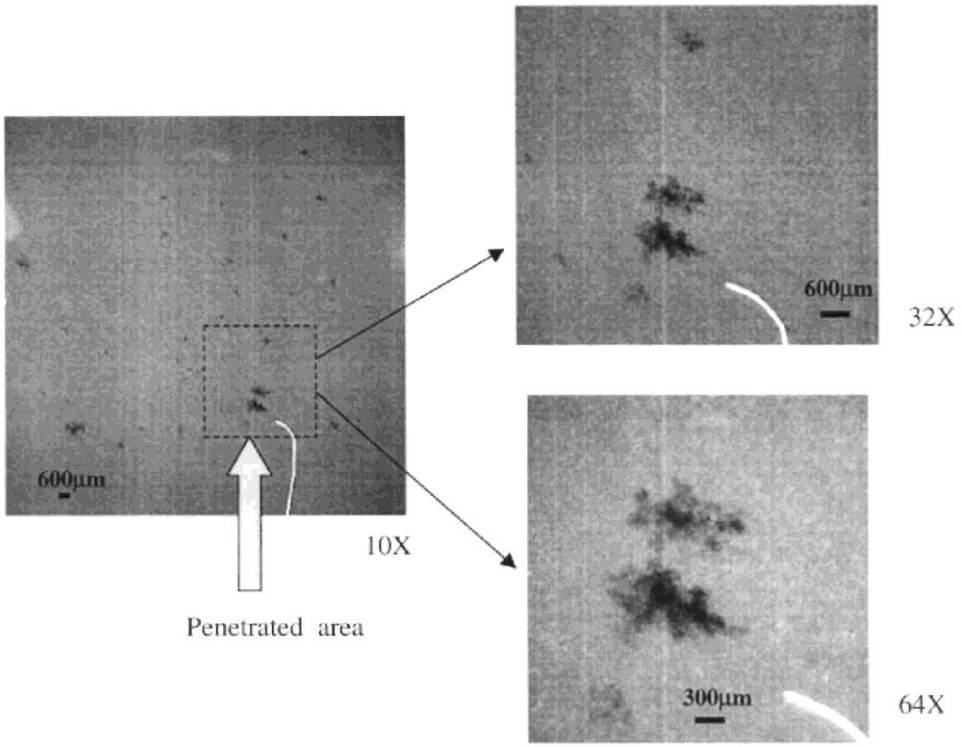

Figure 11. Microradiograph of sample shown in Fig. 10. The bent white line is a lead wire used to mark the position of the penetrated pit.

Impact of this research.—Quantitative measures of pitting resistance traditionally rely on experiments performed under controlled potential or current conditions. The results of this investigation show clearly that the influence of dichromate additions is vastly different at open circuit compared to a potential just 50 mV above open circuit. In order to make open-circuit measurements in a reasonable time, oxidizing agents were added to the solution. The presence of the oxidizers did not change the open-circuit potential appreciably, so the electrode reactions are not vastly different than in the absence of the oxidizer. Only at open circuit or lower potentials is it possible to observe the effects of a cathodic inhibitor.

The foil penetration method provides a measure of the growth rate in the normal direction only. In order to characterize the growth rate and pit shape in the perpendicular direction, it is necessary to use other techniques. Microradiography was shown to be very powerful for characterization of the entire pit shape.

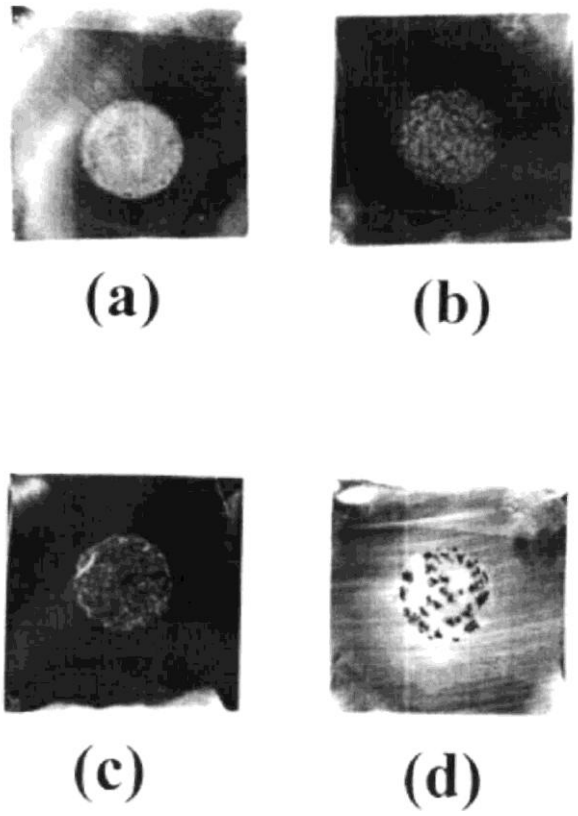

Figure 12. Exposed surface of 0.216 mm thick AA2024-T3 foils potentiostatically pitted at —550 mV SCE exposed to oxygen-stirred solutions of (a) 1 M NaCl, (b) 1 M NaCl + 10^{-3} M $Na_2Cr_2O_7$, (c) 1 M NaCl + 10^{-1} M $Na2Cr_2O_7$, and (d) 1 M NaCl + 1 M $Na2Cr_2O7$. Samples are approximately 1.25 in./3.18 cm squares.

It should be noted that the pH was not constant when dichromate was added in varying amounts in the experiments reported in this study. In fact, the pH decreased with increasing dichromate concentration. This decrease in pH cannot explain the beneficial influence of dichromate, as it is not expected that decreases in pH values below neutral would reduce the tendency for pitting, since Al is amphoteric in nature.

In this work, it is conclusively shown that dichromate ions are cathodic inhibitors. Since pit growth at open circuit is typically under cathodic control, cathodic inhibition should be an effective means for inhibition of pit growth. The results indicate that it may be possible to identify alternate, environmentally friendly inhibitors by their efficacy at cathodic inhibition. In fact, the identification of a critical limiting cathodic current density (or nominal corrosion current density) below which stable pitting does not occur suggests a simple way of testing alternative inhibitors (and the required concentrations). Simple comparison of polarization curves may be a very good predictor of the pitting behavior. However, open-circuit pitting experiments, such as foil penetration measurements, must also be performed.

Conclusions

Foil penetration experiments were performed on AA1100-O and AA2024-T3 in a range of solutions and under different conditions. The following observations were made

1. The pit growth rate in AA2024-T3 at controlled anodic potentials was only slightly

reduced by the addition of as much as 1 M dichromate. However, the pits became more discrete with increasing dichromate concentration in the solution.

2. Dichromate ions at small concentration effectively inhibited open-circuit pit growth and had a large effect on the cathodic portion of polarization curves. Dichromate, or its reduction product, reduces pitting corrosion by acting as a cathodic inhibitor.

3. There appears to be a critical nominal corrosion current density of 20-30 $\mu A/cm^2$ below which stable pitting does not occur.

4. Potentiostatic foil penetration experiments on Al 1100-O showed that pit growth rates increased with increasing applied potential, suggesting that pit growth was under ohmic/charge-transfer control.

5. Pits grown in the short transverse direction in the AA2024-T3 wrought alloy have a convoluted morphology. Microradiographic analysis of penetrated foils provided information on the corrosion attack by detailing pit sizes, shapes, and spatial distribution.

Acknowledgments

The authors thank G. Hodgson and V. Sehgal for helping with the design and construction of the detection circuit. This work was supported by Major H. DeLong at the Air Force Office of Scientific Research, under contract F49620-96-0042.

The Ohio State University assisted in meeting the publication costs of this article.

References

1. F. Hunkeler and H. Böhni, *Corrosion*, **37**, 645 (1981).
2. W. K. Cheung, P. E. Francis, and A. Turnbull, *Mater. Sci. Forum*, **192-194**, Part 1, 185 (1995).
3. B. Zoofan and S. I. Rokhlin, *Mater. Evaluation*, **52**, 191 (1998).
4. H. Böhni and H. H. Uhlig, *J. Electrochem. Soc*., **116**, 906 (1969).
5. A. Sehgal, D. Lu, and G. S. Frankel, *J. Electrochem. Soc*., **145**, 2834 (1998).
6. *ASTM Book of Standards,* Vol. 3.02, Standards G69-81 and G110-92, West Conshohocken, PA (1997).
7. R. Braun, *Werkst. Korros*., **44**, 73 (1993); R. Braun, *Werkst. Korros*., **45**, 255 (1994); and R. Braun, *Werkst. Korros.*, **45**, 369 (1994).
8. S. T. Pride, J. R. Scully, and J. L. Hudson, *J. Electrochem. Soc*., **141**, 3028 (1994).
9. J. Zhao, G. S. Frankel, and R. L. McCreery, *J. Electrochem. Soc*., **145**, 2258 (1998).
10. E. J. Behrman, Private Communication (1998).
11. I. M. Kolthoff and I. K. Miller, *J. Am. Chem. Soc*., **73,** 3055 (1951).
12. E. J. Behrman and J. O. Edwards, *Rev. Inorg. Chem*., **2**, 179 (1980).
13. G. Sussek, M. Kesten, and H.-G. Feller, *Metall. Tech*., **33**, 1031 (1979).